

Journal of Integrated SCIENCE & TECHNOLOGY

An intelligent deep transfer learning platform for accurate classification of multiclass brain tumor

Neelam Khemariya,* Sumit Singh Sonker

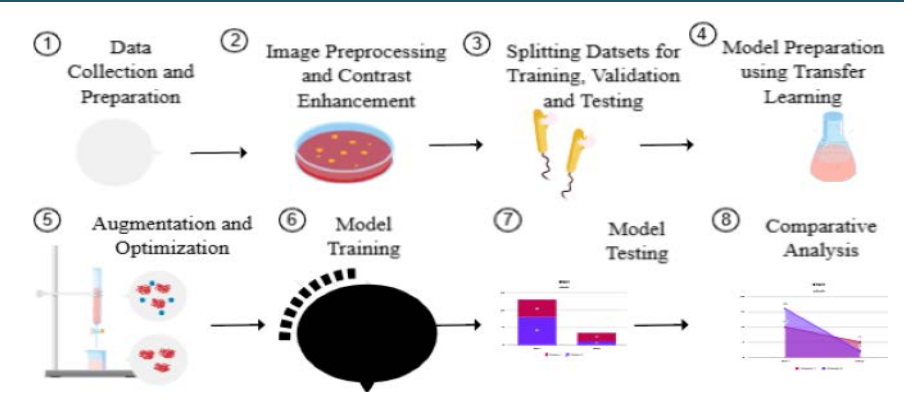
Computer Science and Engineering, Mangalayatan University, Aligarh, Uttar Pradesh, India

Submitted on: 02-Jan-2025, Revised: 08-May-2025, Accepted: 20-May-2025, Published on: 26-May-2025

Article

ABSTRACT

Cancer is the second most common cause of death worldwide after heart disease. If a tumor and its types are identified correctly in the initial phase, it can be treated immediately, and the person's life can be saved. Keeping this in mind, designing and implementing advanced, optimized deep learning models for accurate detection and classification of brain tumors ensures high precision and reliability in diagnostic outcomes and accurate identification of three classes



of brain tumors. A transfer learning mechanism based on human brain MR sample datasets for the severe and efficacious classification of human brain tumors is developed here. The dataset contains samples of four classes of brain MR contrast-enhanced T1-weighted images- glioma tumors, meningioma tumors, pituitary tumors, and no tumors. We enhance the quality and diversity of the brain tumor image dataset through advanced data augmentation techniques and preprocessing methods, ensuring robustness to noise and variability in the input data. After various image preprocessing techniques are applied to enhance the quality and contrast, data augmentation is also used to increase the quantity. We used leverage transfer learning-based feature extraction methods for capturing high-level and relevant features from brain tumor images, enabling efficient representation and improved learning. The model is well trained on 4569 MR images, and its performance is tested on various performance parameters. The proposed model achieved 99.93% accuracy, 99.93% F1–score, 99.93% recall, 99.93% sensitivity, 99.93% average sensitivity, and 99.93% average specificity during training for 100 epochs. It achieved 98.1% accuracy, 98.9% F1 score, 98.3% recall, 98.05% precision, 98.9% sensitivity (average), and 99.4% specificity (average) during testing.

Keywords: Machine Learning, Deep Learning, Transfer Learning, Data Augmentation, DenseNet201, Brain Tumor, Brain MRI Images.

Introduction

Any unwanted growth of tissues or cells inside the brain is termed a brain tumor. When a tumor becomes cancerous, it is called brain cancer. The tumor originating from the brain itself is termed primary, whereas metastatic (secondary) tumors originate from other body parts, such as the kidney, skin, lungs, breast, and colon. Primary tumors are further divided into benign and malignant types. Although it is not easy to detect a brain tumor in the early stages, it has no unique symptoms. Some common symptoms of brain tumors are severe headache, dizziness, personality changes, a

lack of sensation, eye diseases, explanation, or decision-making.² In particular, there is no common cause known for brain tumors.³ However, some causes may include aging, other diseases, various types of tumors, genetics, other dangerous syndromes, or the environment.⁴⁻¹⁰ Whether brain tumors are dangerous or not can be significantly differentiated by their grading. The WHO has classified brain tumors into four grades: 1, 2, 3, and 4. A grade of 1 or 2 indicates that the tumor is not dangerous or noncancerous; grades 3 and 4 indicate that the tumor is dangerous and cancerous. Earlier detection of brain tumors can be performed properly because of the initial stage of diagnosis. Some important scientific techniques used to diagnose tumors are basic neurological tests, CT scans, MRI, MRS, positron emission tomography (PET), and spinal analyses.^{2,9} The advancement of artificial intelligence in terms

Cite as: J. Integr. Sci. Technol., 2025, 13(6), 1142. URN:NBN:sciencein.jist.2025.v13.1142 DOI:10.62110/sciencein.jist.2025.v13.1142



@Authors CC4-NC-ND, ScienceIN https://pubs.thesciencein.org/jist

^{*}Corresponding Author: Neelam Khemariya, Mangalayatan University, India. Email: Neelam.khemariya@gmail.com

of its two most prominent derivatives, machine learning and deep learning, helps it reach every field, including home appliances, medical diagnosis, personal assistance, personal care, the education sector, hospitality, entertainment, chatbots, learning, and many other areas. 11,12 In a traditional learning model, we start from the basics and build a model according to the particular task. This approach takes much time, as we must start from scratch. Transfer learning enables one to perform different tasks via a deep training model, and the performance can be improved for this new task. It allows us to reuse the pretrained previous model and apply it to solve new and different tasks. In the case of a fully connected network, many neurons are needed, as these neurons are associated with every other neuron, which later makes this process tedious and timeconsuming. In the case of images, simple neural networks are ineffective, as they achieve the worst performance due to the number of neurons required and several connections needed. The time and cost complexity increased in managing them. Convolutional neural networks have been developed to solve these problems, especially in the case of image datasets. Owing to their accurate predictions, fast analysis, and precise results, deep transfer learning and other artificial intelligence derivatives are used in various medical diagnosis applications such as heart disease prediction,² segmentation of type 1 and type 2 diabetes disease,³ corn leaf disease detection,⁴ COVID-19 classification,⁵ blood vessel detection ⁶ and various cancer categories such as lung cancer, breast cancer, stomach disease analysis, and mouth cancer.⁷

This paper discusses a transfer learning mechanism based on the fine-tuning of the DenseNet201 architecture applied to a human brain MR image dataset. Initially, we used datasets containing brain MR images from Kaggle and divided them into 3 categories: training, validation, and testing. We then applied preprocessing techniques to these datasets. We then fine-tune DenseNet201 as per our requirements via various modifications and train this transfer learning model on the given datasets as per our requirements. Our final classification model is used for classification purposes. The model will evaluate the input and generate the performance metrics.

PREVIOUS STUDY AND REVIEW OF LITERATURE

A specific type of contusion or lesion in a particular damaged tissue area is known as a brain lesion. In general, all kinds of tumors are lesions, but not all lesions need to be tumors. These brain lesions can occur for various reasons, such as injury, a particular type of stroke, or other factors.³⁰ Noncancerous brain tumors are called benign tumors, and all cancerous tumors are generally known as malignant.³¹ The first case of a brain tumor was detected in 1904, and the great scientist Dr. Alexander Huges Bennet made the first diagnosis. When a tumor originates from some brain tissues, it is treated as primary, whereas a tumor that originates from any other body part and later migrates to the brain is treated as metastatic.³³ Some common symptoms of brain tumors are severe headache in the morning and evening, discomposure or spasm, not comfortable

in thinking, talking, or advertising, change in personality or behavior, frailty or lack of sensation in a particular body part, giddiness or fighting, alteration in appearance or shift in vision, deafness or hearing disorder, facial dullness or emptiness, decision or bafflement, and loss of memory or seafood. Although the actual causes are unknown, some of them may be considered as follows: people aged 65+ have a greater chance of having brain tumors than others do, such as corpulence or Fleshy, the surrounding environment, or the genes of the person. Genetic conditions may also be responsible for the disease, which can be spread through other Syndromes, can be spread from other body parts, and the person has no history of varicella. Brain tumor staging is performed for secondary tumors and is generally not performed for primary tumors because of the size of the tumor. The tumor grade reflects the severity level of the tumor. A lower grade (1 or 2) indicates that the tumor is not dangerous or noncancerous. A higher grade indicates that the tumor is dangerous and cancerous.³⁴ Techniques for the diagnosis of brain tumors include neurological examinations, computed tomography scans, magnetic resonance imaging, magnetic resonance spectroscopy, positron emission tomography, biopsy, and Spinal Tap.

Tseng, C.-J..²¹ proposed a model emanating from particle swarm optimization and extreme gradient boosting transfer learning to diagnose brain tumors properly. As the images are not of good quality, the quality of the images was magnified via the contrast-limited adaptive histogram equalization technique, which is well known for its standard. Image segmentation is achieved via the K-means approach, naïve Bayes approach, and ID3 approach. In previous approaches, PSO ID3 has 86% accuracy, 91% specificity, 90% precision, and 98% recall. The proposed PSOXGBoost model has 97% accuracy, 98% specificity, 97% precision, and 98% recall.

Amran, G.A. et. al.;22 proposed an efficient brain tumor severance technique based on modern ML algorithms known as transfer learning algorithms. This hybrid model adds 14 new layers to the basic GoogleNet model and eliminates the basic 5 layers to enhance the model in such a way that it can be used for automatic feature extraction. It is based on a popular Kaggle dataset known as Br35H. The proposed model has 99% accuracy performance, 99% specificity, 98% precision, 99% F1 score, and 99% recall. The ReLU was modified as the REAF, and the total number of layers reached 33 instead of 22. The proposed model has greater accuracy in differentiating between cancerous and noncancerous images. Samee, N.A. et al., 23 discussed an automated segmentation method based on hybrid rather than traditional machine learning techniques for detecting tumors early, involving manual feature extraction. The model outperforms existing techniques in terms of accuracy and sensitivity, achieving an accuracy of 99.51% and a sensitivity of

Irmak, E.²⁴ provided a CNN-based hybrid architecture that can distinguish different types of brain tumors based on MR images of the human brain. Fine-tuning is employed to modify the transfer learning architecture initially, and the model utilizes the provided weights through a weight optimization technique based on grid search and genetic algorithms. Model testing and validation are subsequently conducted, and it surpasses the GAWO, Xception, and GSWO algorithms in terms of accuracy (99%). The model also

achieved 98% accuracy for ResNet152V2 and 50V2. Islam, Md. M. et. al.²⁵, the authors suggested an architecture based on transfer learning to diagnose brain tumors effectively. The model was applied to four popular CNNs: DenseNet121, VGG19, InceptionV3, and MobileNet. The datasets considered here are brain MR-based images along with three popular and standard datasets - SARTAJ, FIGSHARE, and BR35H - which contain four types of images: Pituitary, Glioma, Meningioma, and No Brain Tumor samples. The model achieves an accuracy of 96% with VGG19, 96% with DenseNet121, 96% with MobileNet, and the best with InceptionV3, which is 98%. The duration of each epoch across all the CNNs was also recorded: 2:44:44 with MobileNet, 3:48:15 with VGG19, 2:50:08 with DenseNet121, and 3:25:08 with InceptionV3.

Dhakshnamurthy, V.K. et. al.; ²⁶, developed a CNN-based hybrid architecture that can distinguish divergent types of brain tumors deployed on brain MR images. The model combines the popular pretrained GoogleNet CNN with a support vector machine for FE and pattern segmentation. The model subsequently integrates this GoogleNet with the SoftMax classifier. Mathivanan, S.K.²⁷, proposed a DL model based on images captured through brain MR images with a GWO with crisp set theory. An unfamiliar dimensionality reduction algorithm with the zestful architecture of multilevel layer modeling in the MLL-CNN) approach. Rasa, S.M et. al.; ²⁸, developed a model composed of a CNN, classifiers, and DL algorithms. The proposed CNN achieved 96.34% accuracy.

MATERIALS AND METHODS

The objectives for the research are outlined below:

Data Enhancement: This enhances the quality and diversity of brain tumor image datasets through advanced data augmentation techniques and preprocessing methods, ensuring robustness to noise and variability in the input data.

Feature Extraction via **Transfer Learning:** Leverage transfer learning-based feature extraction methods for capturing high-level and relevant features from brain tumor images, enabling efficient representation and improved learning.

Deep Learning for Tumor Detection: To design and implement advanced, optimized deep learning models for accurate detection and classification of brain tumors, ensuring high precision and reliability in diagnostic outcomes.

The proposed work presents an approach for classifying multiple classes of brain tumors using an MRI brain dataset through transfer learning. Initially, we utilized datasets containing brain MR images from Kaggle. The dataset is divided into two categories: training and testing. We then applied preprocessing techniques: converting to Grayscale Image, resizing the image to 250x250, standardizing the pixel values, applying CLAHE³⁹, enhancing image quality, normalizing (0--1), and stacking to 3 values. After this, we split the training data into training and validation subsets, at 80% and 20% ratios, respectively. We used a popular CNN, DenseNet201, and fine-tuned it according to our requirements through various modifications. The model was trained on the datasets as per our needs. Training was accomplished by initializing the model, training with real-time augmented data, and validating the model. After loading the model, this trained version is saved and kept in

memory. The final model is used for classification by evaluating the input and generating performance metrics.

The brain tumor dataset considered here is based on human brain magnetic resonance imaging samples, which are free and publicly available. This dataset is the fusion of three datasets - Br35H, Figshare, and SARTAJ. The dataset contains 7023 samples of human brain magnetic resonance images. This dataset contains 4 classes of brain tumor samples: no tumor, glioma tumor, pituitary tumor, and meningioma tumor. Generally, glioma tumors are malignant, but they can also be benign tumors (very few cases). Meningioma tumors are generally benign, but they can also be malignant (very few cases). Pituitary tumors are benign tumors, and the complete taxonomy of the considered dataset is shown in Table 1 below:

Table 1. Complete Taxonomy of the Datasets Containing Human Brain MR Imaging Samples

Samples	Glioma	No	Meningioma	Pituitary
		Tumor		
Training (4569)	1033	1286	1092	1158
Validation (1143)	268	319	291	265
Testing (1311)	300	405	306	300

This dataset can be obtained from https://www.kaggle.com/datasets/masoudnickparvar/brain-tumormri-dataset/data

Image preprocessing techniques are required on the dataset to prepare it for the work requirements. Initially, we converted colorful images into grayscale images because it is a general convention that medical images should be in grayscale for better resolution and dispersion. We standardized the image pixel values so that they have a 0 mean value and a unit standard deviation.

As the quality of the images is not the standard required for our purpose, we have applied a popular contrast enhancement technique called contrast-limited adaptive histogram equalization ⁴⁰. After increasing the contrast at a certain level, we normalize these images by setting the range of these images between 0 and 1 by dividing every image by 255 because the grayscale images lie in the range of 0-255 ⁴². Additionally, we removed the noise from the images to increase the quality. We converted these images into three-channel form because DenseNet201 accepts only three-channel images, and we increased one more parameter. Thus, if the dimension is (225,225), then it will be written as (225,225,1) in three-channel form. As the images are gathered from different places, they are of nonidentical sizes; hence, we need to resize them and store them in the array.

The basic idea behind transfer learning is that the early layer of the deep learning network learns low-level features such as textures or edges and can also be used for other tasks. Therefore, we do not need to train a model again for these basic features, even though we can use transfer learning if the pretrained model has limited datasets and features ⁸. Feature extraction can be achieved via a fixed feature extractor via a pretrained model. It allows less data due to reusability. ⁹. Finally, it is modified in such a way that it maps the

learned features for that specific task. This process is called repurposing.¹⁰ Thus, transfer learning helps generate models with minimal training data, as it can work well without a large amount of data. It also improves the quality by removing overfitting or underfitting on the pretrained model.¹¹ In CNNs, a neuron is not connected with every other neuron, rather, it connects with only a few neurons. This partially connected network arrangement helps reduce the number of parameters and thus speeds up training. The three layers achieve the complete process. The convolutional layer applies a filter on the input provided to it to create a feature map, also called the stack of filter images.¹³ The number of filtered images depends on the filter value set, i.e., if the filter value is set to 10, we obtain 10 filtered images.¹⁴ The feature map is the multiplication of the input image and the feature detector. Here, ReLU removes the values of negative magnitude from the filtered images and replaces them with 0. The image size reduction is achieved by the pooling layer, which is the second layer. The reduction is achieved by choosing a window size and a stride, passing the window across the filter images, and picking the maximum value from each window. In the case of many images, these two layers are applied several times, one by one.¹⁵ The last layer is responsible for image discrimination. Therefore, we can say that it is used for classification. 16 The fully connected layer converts these images into a one-dimensional array for classification.

We considered DenseNet201 as the base model, and the weights were taken from ImageNet. DenseNet201 is an image classification model for handling the vanishing gradient problem. It is used in various medical diagnosis applications, such as COVID-19 prediction ¹⁷ and pneumonia classification. ¹⁸ Thus, the information vanishes before it reaches the output layer, as it needs to travel a very long path. DenseNet overcomes the vanishing gradient problem by connecting each layer with every other layer. DenseNet201 is an important variant of DenseNet, and it is called so because it has 201 layers. 19 The input is directly connected to the 7*7 filter-sized convolutional layer. There are 4 dense blocks: blocks 1, 2, 3, and 4. After every dense block, there is a transition layer. Inside Dense Block 1, we have 6 convolutional layers; inside Dense Block 2, we have 12 convolutional layers; inside Dense Block 3, we have 24 convolutional layers; and in the last Dense Block 4, we have 16 convolutional layers. The down-sampling will be performed only with the transition layer. The convolutional layer inside every dense block has a filter size of 3 by 3 and consists of batch normalization, ReLU, a convolutional layer of 3 by 3, and dropout. DenseNet has several advantages over other existing CNNs. In DenseNet, classifiers use features of all complexities, as they contain the features of all the layers inside a dense block, making them more accurate and efficient. DenseNet also improves the gradient flow during training, as the error signals can be easily shared with the earlier layers of the network, and the information is propagated more efficiently, thus, it solves the problem of gradient descent. In DenseNet, the next layer can easily access the features directly learned by the previous layer inside a dense block, increasing the strength of the propagation of features [20]. The next layer does not need to relearn those features that were already learned by the previous layer, as it can access them directly due to concatenation and saving time.

DenseNet201 has a total of 201 layers. In our proposed model, we keep the initial 151 layers of DenseNet201 unchanged or modified as they are in DenseNet201 and apply fine-tuning to the remaining 50 layers, i.e., layers 152--201. The medical image-specific attention mechanism is achieved by applying the sigmoid activation function on the convolutional 2D layer and then multiplying this attention value onto the inputs of the base model. The sigmoid function [48] is a popular activation function, which looks like S, whose domain is $(-\infty, +\infty)$ and range is (0, +1), and it is expressed as S(x):

$$S(x) = 1/(1 + e^{-x})$$
 (1)

We then applied global average pooling to this. After that, we optimized the dense layer for our task to apply the number of operations on it. Initially, we apply batch normalization, which is used to normalize the images so that they can be in the range of [0-1], and then apply the RELU ⁴⁹, expressed as:

$$f(x) = \max(0, x) \tag{2}$$

Afterwards, the dropout layer is applied so that our model resists overfitting. We then reach the fully connected output layer, where we apply the SoftMax activation function.

Now, we have shaped this model as our modified model. A total of 20824005 parameters (79.44 MB memory occupied) are taken here, of which the trainable parameters are 4389957 (16.75 MB memory occupied) and the nontrainable parameters are 16434048 (62.69 MB memory occupied).

The number of samples increased when augmentation techniques were applied to the dataset. Augmentation is achieved by applying various techniques, such as limited rotation of 15 degrees, a slide shift of 15%, zooming by 15%, and taking the background as black. Table 2 summarizes the different data augmentation parameters and their values.

Table 2. Description of the Data Augmentation Parameters

1	U	
Parameters	Value	Remark
RotationRange	15	Limited Rotation
WidthShiftRange	0.15	Slight Shift in Width
HeightShiftRange	0.15	Slight Shift in Height
FillMode	Constant	Black Background
ZoomRange	0.15	Slight Zoom
HorizontalFlip	True	MRIs can be flipped
cVal	0	Fill value

The model was then compiled via a popular optimizer known as Adam (learning rate of 1e-4), and categorical cross-entropy was used to calculate the loss. Table 3 summarizes the different training parameters and their values.

Table 3. Summarized view of parameters considered for Training

Parameter	Value
Loss	Categorical_Crossentropy
Optimizer	Adam
Learning rate	$1e^{-4}$
Metrics	accuracy
Batch size	10
Epochs	100
Normalization	Yes

EXPERIMENTAL SETUP AND RESULTS

To perform our experiments, we used Google Colab Pro+, which processes very fast due to its background processing capability and can yield results very quickly. For this purpose, we used NVIDIA's Tesla T4 GPU, which is commonly known as the T4 GPU. The use of 25 GB of RAM helped us complete this experiment even faster. The total time to maintain the model was 6318.80 seconds, while the initial and final system memory usage statuses were 28784.277 MB and 35360.9765 MB, respectively.

The proposed model is trained using a batch size of 10 and an epoch size = 100. We also captured traces of the values of loss, validation loss, accuracy, and validation accuracy after every 10 epochs during model training. The total training time taken by the model is 6318.80002 seconds, the initial system memory usage is 28784.277 MB, and the final system memory usage is 35360.9665 MB. The validation of the training of the model is achieved by using numerous parameters of performance with the help of the confusion matrix. It is used to find values by comparing the values between predicted and expected (true) values [50]. These comparisons provide the values of true negative (TN), true positive (TP), false positive (FP), and false negative (FN).

We computed several performance parameters to evaluate the performance of the model.

These parameters are formalized below:

Accuracy = (TN+TP)/(TN+TP+FN+FP)	(3)
Recall = TP/(TP+FN)	(4)
Precision = TP/(TP+FP)	(5)
Specificity = $TN/(TN+FP)$	(6)
F0.5 Score = (P*R)/(P+R)	(7)
Error Rate = $(FN+FP)/(TN+TP+FN+FP)$	(8)
Null Error Rate = $(FP+TN)/(TN+TP+FN+FP)$	(9)
Negative Predicted Value = TN/(TN+FN)	(10)
Balance Accuracy = (TPR+TNR)/2	(11)
Positive False Rate = 1 – Specificity	(12)
Negative False Rate = $1 - Sensitivity$	(13)
False Discovery Rate = 1 – Precision	(14)
False Omission Rate = $FN/(TN+FN)$	(15)
Prevalence = (FN+TP)/(TN+TP+FN+FP)	(16)
Positive Likelihood Ratio = Sensitivity/FPR	(17)
Negative Likelihood Ratio = FNR/Specificity	(18)
Diagnostic Ratio = Pos LR/Neg LR	(19)
$(FM Index)^2 = Precision * Sensitivity$	(20)
Critical success Index = $TP/(TP+FN+FP)$	(21)

The confusion matrix for the training data is represented in Figure 1. The confusion matrix was generated with the support of 1057 glioma tumor samples, 1068 meningioma tumor samples, 1165 pituitary tumor samples, and 1276 nontumor samples.

The classification report is based on the confusion matrix shown in Tables 4 and 5. Our training classification report shows that the proposed model has approximately 100% precision, 100% recall, 100% F1-score, and 100% accuracy for all labeled (glioma, meningioma, pituitary, and no tumor) samples. The figure also

shows a 100% macro average and 100% weighted average for 4569 support samples.

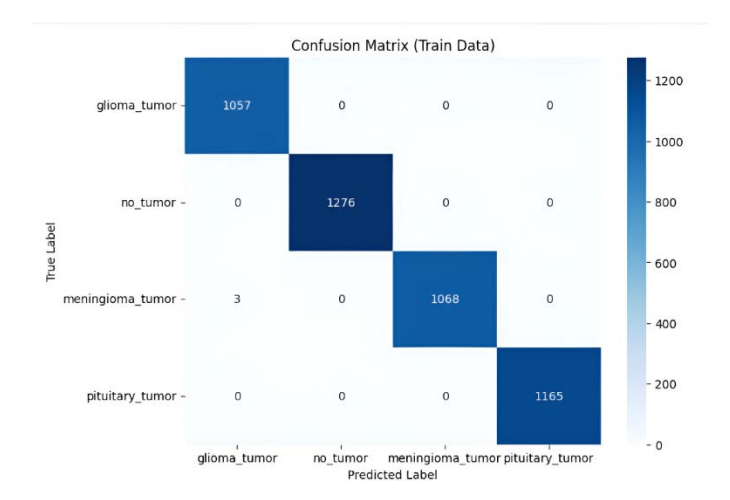


Figure 1. Confusion Matrix for Model Training.

 Table 4. Classification Report for Training data with various performance parameters

Tumor Classes	Precision	Recall	F1- Score	Accuracy
Glioma	0.997	1.000	1.000	0.999
Meningioma	1.000	1.000	0.997	0.999
Pituitary	1.000	1.000	1.000	1.000
No Tumor	1.000	0.997	1.000	1.000

Table 5. Classification Report for Training data with various performance parameters (Averaging)

*				
Type	Precision	Recall	F1- Score	Support
Macro Average	1.0000	1.0000	1.0000	4569
Weighted Average	1.0000	1.0000	1.0000	4569

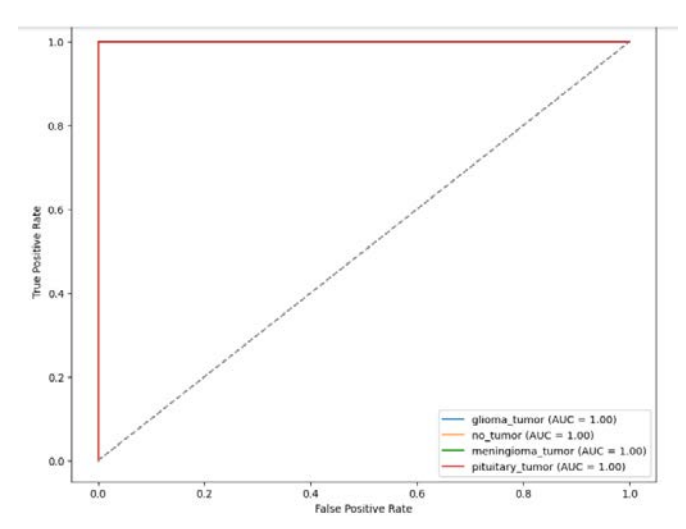


Figure 2. Multiclass ROC curve framed between the TPR and the FPR.

The AUC-ROC curve represents the area under the curve (AUC)-receiver operating characteristic (ROC) curve, which is used to measure the performance of a model on the basis of its TPR

and FPR. The value of the AUC-ROC curve lies between 0 and 1, and the closer it is to 1, the higher the classification performance of the model. If its value is 1, it means that the model can perform 100% accurate classification, but if its value is 50%, then we cannot trust the model at all because, in this case, it is classified randomly. Our AUC-ROC curve shows that its value is almost equal to 1, which means that our model can be used to assess accurately. The multiclass ROC curve is framed between the TPR and the FPR positive rate in Figure 2.

The performance parameters and their predicted values are shown in Table 6. The training performance matrix shows that the proposed model has 99.93% accuracy, 99.93% precision, 99.93% recall, 99.93% F1-score, 99.93% average sensitivity, and 99.97% average specificity.

Table 6. Performance Measurement for Training Data on Various Performance Parameters

Metric	Value Achieved During Training
Accuracy	0.999
Precision	0.999
Recall (Sensitivity)	0.999
F-1 Score	0.999
Average Sensitivity	0.999
Average Specificity	0.999

The relationship between training accuracy and validation accuracy is shown in Figure 3. The training accuracy graph moves toward 1, and the validation accuracy graph lies between 0.95 and 1, indicating that the validation accuracy is greater than 0.95.

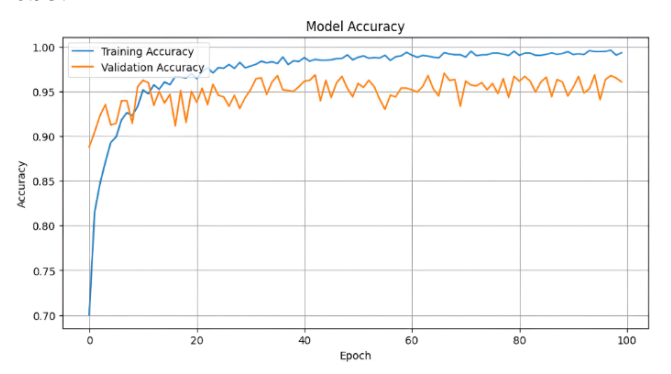


Figure 3. Representation of the graph between Training and Validation Accuracy.

After training, we evaluated the training data via the AUC–ROC curve for each class and then calculated the performance of our model on the basis of popular performance parameters—accuracy, precision, recall, F1 score, average sensitivity, and average specificity and stored these values in the CSV form and then loaded this trained model into our drive. Our model is now ready for testing and evaluation, so testing is performed on 20% of the total images included in our dataset.

The confusion matrix for the test data is represented in Figure 4. The confusion matrix is generated by considering the support of 300 glioma tumor samples, 306 meningioma tumor samples, 300 pituitary tumor samples, and 405 nontumor samples.

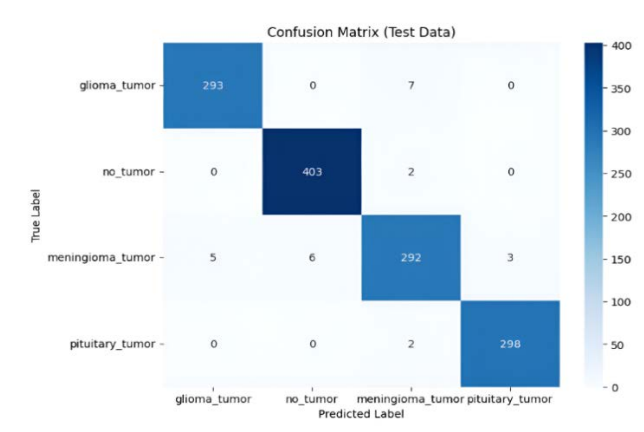


Figure 4. Confusion Matrix for Model Testing.

The classification report is based on the confusion matrix shown in Tables 7 and 8. Our testing classification report shows that the proposed model has approximately 98% precision, 98% recall, 98% F1-score, and 99% accuracy for 300 support samples of glioma tumors. It has approximately 99% precision, 100% recall, 99% F1-score, and 99% accuracy for 405 support samples of no tumors. It has approximately 96% precision, 95% recall, 96% F1-score, and 98% accuracy for 306 support samples of meningioma tumors. It has approximately 99% precision, 99% recall, 99% F1-score, and 99.6% accuracy for 300 support samples of tumors (Table 7). It has a 98% macro average and weighted average for precision, recall, and F1-score on 1311 support samples (Table 8).

 Table 7. Classification Report for Testing data with various performance parameters

Tumor Classes	Precision	Recall	F1- Score	Accuracy
Glioma	0.983	0.977	0.979	0.991
Meningioma	0.964	0.954	0.959	0.981
Pituitary	0.990	0.993	0.992	0.996
No Tumor	0.985	0.995	0.989	0.994

 Table 8. Classification Report for Testing data with various performance parameters (Averaging)

Type	Precision	Recall	F1- Score	Support
Macro Average	0.98	0.98	0.98	1311
Weighted Average	0.98	0.98	0.98	1311

The performance parameters and their predicted values are shown in Table 9. The testing performance matrix shows that the proposed model has 98.1% accuracy, 98.5% precision, 98.3% recall, 98.2% F1-score, 98.9% average sensitivity, and 99.4% average specificity.

Table 9. Performance Measurement for Testing Data on Various Performance Parameters

Metric	Value Achieved During Training
Accuracy	0.981
Precision	0.985
Recall (Sensitivity)	0.983
F-1 Score	0.982
Average Sensitivity	0.989
Average Specificity	0.994

PERFORMANCE MEASUREMENT AND COMPARATIVE ANALYSIS

On the basis of the confusion matrix generated from testing the model, we computed the values of the abovementioned performance parameters for glioma tumors, meningioma tumors, pituitary tumors, and no tumors, using the values of true negatives (TN), true positives (TP), false negatives (FN), and false positives (FP). The values of true negative, true positive, false negative, and false positive for all four classes are shown in Table 10.

Table 10. Measured values of TP, FP, TN, and FN for the testing classification matrix

Tumor	TP	TN	FP	FN	
Classes					
Glioma	293	1006	5	7	
Meningioma	292	994	6	2	
Pituitary	298	1008	3	2	
No Tumor	403	900	6	2	

On the basis of the values of TP, FP, TN, and FN, we computed the values of the performance parameters, which are shown in Table 11.

Table 11. Measured Values of Various Performance Parameters

Performance	Glioma	No	Mening	Pituitar
Parameter	Tumor	Tumor	ioma	y
			Tumor	Tumor
Error Rate	0.0091	0.0061	0.0190	0.0038
Specificity	0.9950	0.9933	0.9890	0.9970
Null Error Rate	0.7711	0.6910	0.7665	0.7711
Prevalence	0.2288	0.3089	0.2334	0.2288
False Positive Ratio	0.005	0.0067	0.011	0.003
False Negative Ratio	0.0234	0.0050	0.0458	0.0067
False Discovery Rate	0.0168	0.0.0147	0.364	0.01
Negative Predicted	0.9930	0.9977	0.9861	0.9980
Value				
False Omission Rate	0.0069	0.0022	0.0138	0.0019
Positive Likelihood	195.32	148.507	86.74	331.1
Ratio				
Negative Likelihood	0.0235	0.0050	0.0463	0.0067
Ratio				
Critical Success Index	0.9606	0.9805	0.9211	0.9834
Balanced Accuracy	0.9858	0.9941	0.9716	0.9951
FM Index	0.9798	0.9901	0.9588	0.9916
BM	0.9716	0.9833	0.9432	0.9903
MK	0.9762	0.9830	0.9497	0.988

A quantified analysis of the suggested model with underlying approaches established on various performance parameters is shown in Tables 12–15. We performed a comparative analysis of our proposed model with existing models for all four classes, i.e., glioma tumors, meningioma tumors, pituitary tumors, and no tumors. We also performed a comparative analysis of the overall performance of the proposed model in terms of accuracy, recall, precision, and F1 score parameters with that of existing models and

Table 12. Multiclass Comparison of Testing results (Glioma tumor) of the proposed model regarding various performance benchmarks with Existing Models

#	Year	Precision	Recal	F1- Score	Accuracy
			l		
[24]	2021	0.934	0.944	-	0.979
[28]	2024	0.990	0.960	0.970	0.982
[38]	2024	0.990	0.940	0.960	0.980
Propo		0. 983	0.977	0.979	0.9908
sed					

Table 13. Multiclass Comparison of Testing results (Meningioma tumor) of the proposed model regarding various performance benchmarks with Existing Models

#	Year	Precision	Recall	F1- Score	Accuracy
[24]	2021	0.923	0.924	-	0.976
[28]	2024	0.965	0.950	0.960	0.981
[38]	2024	0.940	0.986	0.950	0.980
Proposed	d	0.964	0.954	0.960	0.981

Table 14. Multiclass Comparison of Testing results (Pituitary tumor) of the proposed model regarding various performance benchmarks with Existing Models

#	Year	Precision	Recal	F1- Score	Accuracy
			l		
[24]	2021	0.909	0.880	-	0.969
[28]	2024	0.960	0.990	0.970	0.982
[38]	2024	0.970	0.990	0.980	0.980
Proposed		0.990	0.993	0.992	0.996

Table 15. Multiclass Comparison of Testing Results (No tumor) of the Proposed Model Regarding Various Performance Benchmarks with Existing Models

#	Year	Precision	Recall	F1-	Accuracy
				Score	
[24]	2021	0.880	0.921	-	0.954
[28]	2024	0.970	0.990	0.980	0.982
[38]	2024	1.000	1.000	1.000	0.980
Proposed		0.985	0.996	0.989	0.994

find that our proposed model outperforms other models in terms of several parameters. Table 16 shows the comparison between the proposed model and the existing model on the basis of the accuracy parameter. Table 17 shows the comparison between the proposed model and the existing model on the basis of the recall parameter. Table 18 shows the comparison between the proposed model and the existing model on the basis of the specificity parameter. Table 19 shows the comparison between the proposed model and the existing model on the basis of the F1 score. Table 20 shows the comparison between the proposed model and the existing model on the basis of the precision parameter.

Table 16. Comparison of the Accuracy parameters between the suggested and underlying models

Approach	Year	Accuracy (%)
[21]	2023	97
[28]	2024	96.34
[38]	2024	98
<u>[41]</u>	2024	85.99
[46]	2023	87.9
[47]	2022	96
[52]	2023	93.44
[53]	2023	92.45
[54]	2023	97.95
Proposed		98.09

Table 17. Comparison of the Recall parameters between the suggested and underlying models

Approach	Year	Recall (%)
[21]	2023	98
[22]	2024	98.6
[32]	2024	97.08
[35]	2024	97.11
<u>[46]</u>	2023	92.3
[47]	2022	96
[52]	2023	95.75
[53]	2023	96.3
Proposed		98.09

Table 18. Comparison of the Specificity parameters between the suggested and underlying models

Approach	Year	Specificity (%)
[21]	2023	98
[24]	2022	98
[46]	2023	73.65
[53]	2023	98.76
Proposed		99.37

Table 19. Comparison of the F1 Score parameters between the suggested and underlying models

Approach	Year	F1- Score (%)
[21]	2023	98
[35]	2024	97.08
[47]	2022	95.7
[52]	2023	95
[53]	2023	96.3
Proposed		98.08

Table 20. Comparison of the precision parameters between the suggested and underlying models

Approach	Year	Precision (%)
[21]	2023	97
[22]	2024	98.9
[23]	2022	99
[35]	2024	98.05
[47]	2022	96
[50]	2022	97.7
[51]	2023	98

[52]	2023	94.75	
[53]	2023	96.3	
Proposed		98.08	

We measured the performance of our proposed model on the basis of various parameters for all four classes: glioma tumor, meningioma tumor, pituitary tumor, and no tumor. Our model achieves the highest performance for almost all the parameters, and the performance of the proposed model is better than that of the existing models for almost all the performance parameters considered. Comparative analysis reveals that our model has good accuracy, recall, F1 score, and specificity compared with the existing models. However, the possibility of enhancing these parameters, specifically the precision parameter, is possible.

CONCLUSION

In this paper, we suggest a transfer learning approach using finetuned DenseNet201 Convolutional Neural Networks based on Hunan Brain Magnetic Resonance Imaging Datasets for the effective and efficient severity and classification of brain tumors. The dataset is composed of 4 types of samples - No tumor, glioma, pituitary, and meningioma—and is divided into three parts training, validation, and testing-and contains 4569, 1142, and 1311 image samples for training, validation, and testing, respectively. Various image preprocessing approaches, such as grayscale and three-channel conversion, are used to amplify the status and contrast of the images and resize them. Data augmentation techniques are used to expand the dataset samples. Fine-tuning was applied to DenseNet201's last 50 layers while taking the weights from ImageNet. The model is well trained via optimizers with accuracy metrics, and its performance is validated and tested on various performance parameters. The model achieved 99.93% accuracy, 99.93% precision, 99.93% recall, 99.93% F1 score, 99.93% average sensitivity, and 99.93% average specificity during training for 100 epochs. During testing, our model achieved an overall 98.1% accuracy, 98.5% precision, 98.3% recall, 98.9% F1 score, 98.9% average sensitivity, and 99.4% average specificity. We also compared the performance of our proposed model for all four classes separately with that of the existing models, which showed better performance in terms of the number of parameters.

In the future, we will also attempt hybrid approaches to enhance the dataset by combining more publicly available datasets and applying transfer learning more efficiently and accurately to the fusion of two or more convolutional neural networks. We will also integrate explainable AI techniques, such as SHAP or LIME, to provide interpretable results, highlight critical regions of interest, and offer insights into model decision-making processes. Additionally, we will incorporate mechanisms for assessing the severity of detected brain tumors, facilitating better clinical decision-making and treatment planning. We will also attempt to implement a secure cloud-based infrastructure for storing processed data, model outputs, and results, ensuring seamless accessibility and scalability for future applications.

ACKNOWLEDGMENTS

We acknowledge all the support received from Mangalayatan University, India.

CONFLICT OF INTEREST STATEMENT

The authors declare that they have no relevant financial or nonfinancial interests to disclose and no funds, grants, or other support were received during the preparation of this manuscript.

DATA AVAILABILITY STATEMENT

The datasets analyzed during the current study are available at:

https://www.kaggle.com/datasets/masoudnickparvar/braintumor-mri-dataset/data

REFERENCES

- Shaikh, T. A., Rasool, T., Verma, P., & Mir, W. A. (2024). A fundamental overview of ensemble deep learning models and applications: systematic literature and state of the art. *Annals of Operations Research*. https://doi.org/10.1007/s10479-024-06444-0.
- Rana, M., & Bhushan, M. (2023). Machine learning and deep learning approach for medical image analysis: diagnosis to detection. *Multimedia Tools and Applications*, 82(17), 26731–26769. https://doi.org/10.1007/s11042-022-14305-w
- Richens, J. G., Lee, C. M., & Johri, S. (2020). Improving the accuracy of medical diagnosis with causal machine learning. *Nature Communications*, 11(1), 3923. https://doi.org/10.1038/s41467-020-17419-7.
- 4 Aakanksha, M. (2023). Brain Tumor Detection using Deep Learning. International Journal for Research in Applied Science and Engineering Technology, 11(7), 490–493. https://doi.org/10.22214/ijraset.2023.54665
- Joshi, K. K., Gupta, K., & Agrawal, J. (2023). An efficient transfer learning approach for prediction and classification of SARS COVID -19.
 Multimedia Tools and Applications, 83(13), 39435–39457. https://doi.org/10.1007/s11042-023-17086-y.
- dos Santos, J. C. M., Carrijo, G. A., de Fátima dos Santos Cardoso, C., Ferreira, J. C., Sousa, P. M., & Patrocínio, A. C. (2020). Fundus image quality enhancement for blood vessel detection via a neural network using CLAHE and Wiener filter. *Research on Biomedical Engineering*, 36(2), 107–119. https://doi.org/10.1007/s42600-020-00046-y.
- 7. Wee, B. F., Sivakumar, S., Lim, K. H., Wong, W. K., & Juwono, F. H. (2023). Diabetes detection based on machine learning and deep learning approaches. *Multimedia Tools and Applications*, 83(8), 24153–24185. https://doi.org/10.1007/s11042-023-16407-5
- Singh, N., & Jaiswal, U. C. (2024a). Sentiment classification on product reviews using machine learning and deep learning techniques. *International Journal of System Assurance Engineering and Management*, 15(12), 5726–5741. https://doi.org/10.1007/s13198-024-02592-5.
- Ahmed, S. F., Alam, Md. S. bin, Hassan, M., Rozbu, M. R., Ishtiak, T., Rafa, N., Mofijur, M., Shawkat Ali, A. B. M., & Gandomi, A. H. (2023). Deep learning modelling techniques: current progress, applications, advantages, and challenges. *Artificial Intelligence Review*, 56(11), 13521–13617. https://doi.org/10.1007/s10462-023-10466-8
- 10.Getman, A. I., Rybolovlev, D. A., & Nikolskaya, A. G. (2024). Deep Learning Applications for Intrusion Detection in Network Traffic. Programming and Computer Software, 50(7), 493–510. https://doi.org/10.1134/S0361768824700221.
- 11.AKMEŞE, Ö. F. (2024). Data privacy-aware machine learning approach in pancreatic cancer diagnosis. *BMC Medical Informatics and Decision Making*, 24(1), 248. https://doi.org/10.1186/s12911-024-02657-2.
- 12.Janiesch, C., Zschech, P., & Heinrich, K. (2021). Machine learning and deep learning. *Electronic Markets*, 31(3), 685–695. https://doi.org/10.1007/s12525-021-00475-2.
- 13.Irene, D. S., Peter, J. S. P., Sankarasubramanian, N., & Krishnakanth, S. P. (2025). EHRT-RWB: A Novel Ensemble Hybrid Recurrent Transformer for

- Multimodal Heart Disease Risk Prediction. *Journal of The Institution of Engineers* (*India*): Series B, 106(2), 475–486. https://doi.org/10.1007/s40031-024-01085-0.
- 14.Khan, A., Sohail, A., Zahoora, U., & Qureshi, A. S. (2020). A survey of the recent architectures of deep convolutional neural networks. *Artificial Intelligence Review*, 53(8), 5455–5516. https://doi.org/10.1007/s10462-020-09825-6.
- 15.Ersavas, T., Smith, M. A., & Mattick, J. S. (2024). Novel applications of Convolutional Neural Networks in the age of Transformers. *Scientific Reports*, 14(1), 10000. https://doi.org/10.1038/s41598-024-60709-z.
- 16.Taye, M. M. (2023). Theoretical Understanding of Convolutional Neural Network: Concepts, Architectures, Applications, Future Directions. Computation, 11(3), 52. https://doi.org/10.3390/computation11030052.
- 17.Hasan, N., Bao, Y., Shawon, A., & Huang, Y. (2021). DenseNet Convolutional Neural Networks Application for Predicting COVID-19 Using CT Image. SN Computer Science, 2(5), 389. https://doi.org/10.1007/s42979-021-00782-7.
- 18.Sivasubramaniam, S., & Balamurugan, S. P. (2024). Early detection and prediction of Heart Disease using Wearable devices and Deep Learning algorithms. *Multimedia Tools and Applications*, 84(9), 6187–6201. https://doi.org/10.1007/s11042-024-19127-6.
- 19.Hou, Y., Wu, Z., Cai, X., & Zhu, T. (2024). The application of improved densenet algorithm in accurate image recognition. *Scientific Reports*, 14(1), 8645. https://doi.org/10.1038/s41598-024-58421-z.
- 20.Yin, L., Hong, P., Zheng, G., Chen, H., & Deng, W. (2022). A Novel Image Recognition Method Based on DenseNet and DPRN. Applied Sciences, 12(9), 4232. https://doi.org/10.3390/app12094232.
- 21.Tseng, C.-J., & Tang, C. (2023). An optimized XGBoost technique for accurate brain tumor detection using feature selection and image segmentation. *Healthcare Analytics*, 4, 100217. https://doi.org/10.1016/j.health.2023.100217.
- 22.Amran, G. A., Alsharam, M. S., Blajam, A. O. A., Hasan, A. A., Alfaifi, M. Y., Amran, M. H., Gumaei, A., & Eldin, S. M. (2022). Brain Tumor Classification and Detection Using Hybrid Deep Tumor Network. *Electronics*, 11(21), 3457. https://doi.org/10.3390/electronics11213457.
- 23.Samee, N. A., Mahmoud, N. F., Atteia, G., Abdallah, H. A., Alabdulhafith, M., Al-Gaashani, M. S. A. M., Ahmad, S., & Muthanna, M. S. A. (2022). Classification Framework for Medical Diagnosis of Brain Tumor with an Effective Hybrid Transfer Learning Model. *Diagnostics*, 12(10), 2541. https://doi.org/10.3390/diagnostics12102541.
- 24.Irmak, E. (2021). Multi-Classification of Brain Tumor MRI Images Using Deep Convolutional Neural Network with Fully Optimized Framework. Iranian Journal of Science and Technology, Transactions of Electrical Engineering, 45(3), 1015–1036. https://doi.org/10.1007/s40998-021-00426-9.
- 25.Islam, Md. M., Barua, P., Rahman, M., Ahammed, T., Akter, L., & Uddin, J. (2023). Transfer learning architectures with fine-tuning for brain tumor classification using magnetic resonance imaging. *Healthcare Analytics*, 4, 100270. https://doi.org/10.1016/j.health.2023.100270.
- 26.Dhakshnamurthy, V. K., Govindan, M., Sreerangan, K., Nagarajan, M. D., & Thomas, A. (2024). Brain Tumor Detection and Classification Using Transfer Learning Models. *CC* 2023, 1. https://doi.org/10.3390/engproc2024062001.
- 27. Mathivanan, S. K., Sonaimuthu, S., Murugesan, S., Rajadurai, H., Shivahare, B. D., & Shah, M. A. (2024). Employing deep learning and transfer learning for accurate brain tumor detection. *Scientific Reports*, 14(1), 7232. https://doi.org/10.1038/s41598-024-57970-7.
- 28.Rasa, S. M., Islam, Md. M., Talukder, Md. A., Uddin, Md. A., Khalid, M., Kazi, M., & Kazi, Md. Z. (2024). Brain tumor classification using fine-tuned transfer learning models on magnetic resonance imaging (MRI) images. DIGITAL HEALTH, 10. https://doi.org/10.1177/20552076241286140.
- 29.Kumar, K., Jyoti, K., & Kumar, K. (2024). Machine learning for brain tumor classification: evaluating feature extraction and algorithm efficiency. *Discover Artificial Intelligence*, 4(1), 112. https://doi.org/10.1007/s44163-024-00214-4.

- 30.Kaifi, R. (2023). A Review of Recent Advances in Brain Tumor Diagnosis Based on AI-Based Classification. *Diagnostics*, 13(18), 3007. https://doi.org/10.3390/diagnostics13183007.
- 31.Reichenbach, M., Richter, S., Galli, R., Meinhardt, M., Kirsche, K., Temme, A., Emmanouilidis, D., Polanski, W., Prilop, I., Krex, D., Sobottka, S. B., Juratli, T. A., Eyüpoglu, I. Y., & Uckermann, O. (2024). Clinical confocal laser endomicroscopy for imaging of autofluorescence signals of human brain tumors and non-tumor brain. *Journal of Cancer Research and Clinical Oncology*, 151(1), 19. https://doi.org/10.1007/s00432-024-06052-2.
- 32.Khaliki, M. Z., & Başarslan, M. S. (2024). Brain tumor detection from images and comparison with transfer learning methods and 3-layer CNN. *Scientific Reports*, 14(1), 2664. https://doi.org/10.1038/s41598-024-52823-9.
- 33.Mahmud, M. I., Mamun, M., & Abdelgawad, A. (2023). A Deep Analysis of Brain Tumor Detection from MR Images Using Deep Learning Networks. *Algorithms*, 16(4), 176. https://doi.org/10.3390/a16040176.
- 34.Bogacsovics, G., Harangi, B., & Hajdu, A. (2024). Developing diverse ensemble architectures for automatic brain tumor classification. *Multimedia Tools and Applications*. https://doi.org/10.1007/s11042-024-19657-z.
- 35.A.G, B., Srinivasan, S., D, P., P, M., Mathivanan, S. K., & Shah, M. A. (2024). Robust brain tumor classification by fusion of deep learning and channel-wise attention mode approach. *BMC Medical Imaging*, 24(1), 147. https://doi.org/10.1186/s12880-024-01323-3.
- 36.Hao, R., Namdar, K., Liu, L., & Khalvati, F. (2021). A Transfer Learning–Based Active Learning Framework for Brain Tumor Classification. Frontiers in Artificial Intelligence, 4. https://doi.org/10.3389/frai.2021.635766.
- 37. Van Dieren, L., Amar, J. Z., Geurs, N., Quisenaerts, T., Gillet, C., Delforge, B., D'heysselaer, L. D. C., Filip Thiessen, E., Cetrulo, C. L., & Lellouch, A. G. (2023). Unveiling the power of convolutional neural networks in melanoma diagnosis. *European Journal of Dermatology*, 33(5), 495–505. https://doi.org/10.1684/ejd.2023.4559
- 38.Matin Malakouti, S., Bagher Menhaj, M., & Abolfazl Suratgar, A. (2024). Machine learning and transfer learning techniques for accurate brain tumor classification. *Clinical EHealth*, 7, 106–119. https://doi.org/10.1016/j.ceh.2024.08.001.
- 39.Tenghongsakul, K., Kanjanasurat, I., Archevapanich, T., Purahong, B., & Lasakul, A. (2023). Deep transfer learning for brain tumor detection based on MRI images. *Journal of Physics: Conference Series*, 2497(1), 012015. https://doi.org/10.1088/1742-6596/2497/1/012015.
- 40.Babu Vimala, B., Srinivasan, S., Mathivanan, S. K., Mahalakshmi, Jayagopal, P., & Dalu, G. T. (2023). Detection and classification of brain tumor using hybrid deep learning models. *Scientific Reports*, 13(1), 23029. https://doi.org/10.1038/s41598-023-50505-6.
- 41.Rustom, F., Moroze, E., Parva, P., Ogmen, H., & Yazdanbakhsh, A. (2024).

 Deep learning and transfer learning for brain tumor detection and classification. *Biology Methods and Protocols*, 9(1). https://doi.org/10.1093/biomethods/bpae080.
- 42.ZainEldin, H., Gamel, S. A., El-Kenawy, E.-S. M., Alharbi, A. H., Khafaga, D. S., Ibrahim, A., & Talaat, F. M. (2022). Brain Tumor Detection and Classification Using Deep Learning and Sine-Cosine Fitness Grey Wolf Optimization. *Bioengineering*, 10(1), 18. https://doi.org/10.3390/bioengineering10010018.

- 43.Yurtsever, M. M. E., Atay, Y., Arslan, B., & Sagiroglu, S. (2024). Development of brain tumor radiogenomic classification using GAN-based augmentation of MRI slices in the newly released gazi brains dataset. BMC Medical Informatics and Decision Making, 24(1), 285. https://doi.org/10.1186/s12911-024-02699-6
- 44.Srinivas, C., K. S., N. P., Zakariah, M., Alothaibi, Y. A., Shaukat, K., Partibane, B., & Awal, H. (2022). Deep Transfer Learning Approaches in Performance Analysis of Brain Tumor Classification Using MRI Images. *Journal of Healthcare Engineering*, 2022, 1–17. https://doi.org/10.1155/2022/3264367.
- 45. Yaqub, M., Feng, J., Zia, M., Arshid, K., Jia, K., Rehman, Z., & Mehmood, A. (2020). State-of-the-Art CNN Optimizer for Brain Tumor Segmentation in Magnetic Resonance Images. *Brain Sciences*, 10(7), 427. https://doi.org/10.3390/brainsci10070427.
- 46. Aggarwal, M., Tiwari, A. K., Sarathi, M. P., & Bijalwan, A. (2023). An early detection and segmentation of Brain Tumor using Deep Neural Network. BMC Medical Informatics and Decision Making, 23(1), 78. https://doi.org/10.1186/s12911-023-02174-8
- 47.Girdhar, N., Sinha, A., & Gupta, S. (2023). DenseNet-II: an improved deep convolutional neural network for melanoma cancer detection. *Soft Computing*, 27(18), 13285–13304. https://doi.org/10.1007/s00500-022-07406-z.
- 48.Martínez-Del-Río-Ortega, R., Civit-Masot, J., Singh-Perejón, F., & Domínguez-Morales, M. (2024). Brain Tumor Detection Using Magnetic Resonance Imaging and Convolutional Neural Networks. Big Data and Cognitive Computing, 8(9), 123. https://doi.org/10.3390/bdcc8090123
- 49.Sailunaz, K., Bestepe, D., Alhajj, S., Özyer, T., Rokne, J., & Alhajj, R. (2023). Brain tumor detection and segmentation: Interactive framework with a visual interface and feedback facility for dynamically improved accuracy and trust. *PLOS ONE*, *18*(4), e0284418. https://doi.org/10.1371/journal.pone.0284418.
- 50.Archana, K. v., & Komarasamy, G. (2023). A novel deep learning-based brain tumor detection using the Bagging ensemble with K-nearest neighbor. *Journal of Intelligent Systems*, 32(1). https://doi.org/10.1515/jisys-2022-0206.
- 51.Ramtekkar, P. K., Pandey, A., & Pawar, M. K. (2023). Accurate detection of brain tumor using optimized feature selection based on deep learning techniques. *Multimedia Tools and Applications*, 82(29), 44623–44653. https://doi.org/10.1007/s11042-023-15239-7.
- 52.Saeedi, S., Rezayi, S., Keshavarz, H., & R. Niakan Kalhori, S. (2023). MRI-based brain tumor detection using convolutional deep learning methods and chosen machine learning techniques. *BMC Medical Informatics and Decision Making*, 23(1), 16. https://doi.org/10.1186/s12911-023-02114-6.
- 53.Sarkar, A., Maniruzzaman, Md., Alahe, M. A., & Ahmad, M. (2023). An Effective and Novel Approach for Brain Tumor Classification Using AlexNet CNN Feature Extractor and Multiple Eminent Machine Learning Classifiers in MRIs. *Journal of Sensors*, 2023(1). https://doi.org/10.1155/2023/1224619.
- 54.Sawle A, Bhosale S. (2023). Brain tumor detection using deep learning. *Int J Res App Sci Engg*, 11(7), 490-494. https://doi.org/10.22214/ijraset.2023.54665.